

Morphology and Hydrogen-Bond Restricted Crystallization of Poly(butylene succinate)/Cellulose Diacetate Blends

Weihoa Zhou, Shuaishuai Yuan, Yiwang Chen, Le Bao

Institute of Polymers, Nanchang University, 999 Xuefu Avenue, Nanchang 330031, China

Received 28 April 2011; accepted 27 July 2011

DOI 10.1002/app.35351

Published online 3 November 2011 in Wiley Online Library (wileyonlinelibrary.com).

ABSTRACT: Poly(butylene succinate)/cellulose diacetate (PBS/CDA) blends were prepared by the solution blending method from poly(butylene succinate) (PBS) and cellulose diacetate (CDA). The influence of hydrogen bond on the structure, morphology, crystallization, as well as the physical properties of PBS/CDA blends was significantly investigated. The fourier transform infrared spectroscopy (FTIR) results indicated that the carbonyl groups of PBS shifted to higher wavenumbers and disappeared at the content of 60% CDA, due to the formation of hydrogen bond between PBS and CDA. The wide-angle X-ray diffractometer (WAXD) and differential scanning calorimeter (DSC) analysis suggest that the crystallization of PBS was significantly restricted by the incorporation of CDA, which

is also attributed to the hydrogen bonding. The scanning electron microscope (SEM) and polarized optical microscopy (POM) results revealed that PBS and CDA were miscible without appearance of obvious phase separation. The hydrogen bonding interaction led to the change of decomposing mechanism of blends as determined by thermogravimetric analysis (TGA), as well as the increase of the elongation at break due to the reduced crystallinity of PBS. The existence of CDA led to the decrease of water contact angle, showing of the improved hydrophilicity. © 2011 Wiley Periodicals, Inc. *J Appl Polym Sci* 124: 3124–3131, 2012

Key words: poly(butylene succinate); cellulose; blend; crystallization

INTRODUCTION

The use of renewable sources for both polymer matrices and reinforcement material offers an answer to maintaining sustainable development of economically and ecologically attractive structural composite technology.¹ Polymer blending with natural polymers has attracted a great attention for the development of new polymeric materials, since the properties of natural polymers can be significantly improved by blending with the counter polymers.²

The aliphatic polyester of poly(butylene succinate) (PBS) is one of the most promising materials for the production of high-performance, environmentally friendly, biodegradable materials.^{3–5} PBS could be produced from renewable resources, showing of the melting point similar to that of low density polyethylene (LDPE) and tensile strength between PE and

polypropylene (PP), as well as excellent processing capabilities.⁶ However, the crystalline PBS is brittle due to its relatively high crystallinity, and some methods such as adding the additive, inorganic filler, nanocomposite, and other polymers were developed to modify the properties.^{7–12}

Cellulose as one of the biodegradable and renewable resource, is the most abundant raw material in the world.^{13,14} And the cellulose derivatives are an intriguing polymer component to be blended with polymers, since they can be obtained from cellulose materials. Cellulose esters exhibit a fairly high glass transition temperature (T_g), good clarity, high flexural, and tensile strengths. Moreover, they are potentially biodegradable,^{15–18} and they could be used in a broad field of applications such as coatings, optical films, composites, and biodegradable plastics. Cellulose diacetate (CDA) is one of important cellulose derivatives, and made from resources. Some of the three OH groups in a glucose unit of cellulose are substituted for $-OCOCH_3$ groups. CDA films have a tensile strength comparable to polystyrene. Some researchers have reported that CDA could act as a plasticizer for some polyesters, such as poly(vinyl alcohol)¹⁹ and PLA.^{20,21} Uesaka et al.^{22,23} found that the PBS and cellulose triacetate (CTA) were compatible and the CTA restricted the degradation of PBS. Tachibana et al.²⁴ found that the cellulose acetate butyrate (CAB) could increase the elongation at break while maintain the tensile strength of PBS.

Correspondence to: W. Zhou (dramzwh@126.com) and Y. Chen (ywchen@ncu.edu.cn).

Contract grant sponsor: Natural Science Foundation of Jiangxi Province; contract grant number: 2009GQH0068.

Contract grant sponsor: Jiangxi Provincial Department of Education, Program for Production, Education and Research; contract grant number: GJJ10004.

Contract grant sponsor: Program for Innovative Research Team in University of Jiangxi Province.

In general, the cellulose esters tended to deteriorate the crystallization of PBS, leading to the formation of amorphous blends based on PBS. Most of the researchers just discussed about the special interaction between PBS and the cellulose derivatives. However, they did not mention the hydrogen bonding interaction between the components. Recently, Hashimoto et al.²⁵ investigated the effect of intermolecular hydrogen bondings on isothermal crystallization behavior of polymer blends of cellulose acetate butyrate and poly(3-hydroxybutyrate). Furthermore, the miscibility and morphology in the PBS and cellulose derivatives blends still remain to be extensively studied.

Because of the biodegradability of CDA, the blending of CDA with PBS leads to the formation of novel blends based on biorenewable resources. The interaction of hydroxyl groups in CDA and carbonyl groups in PBS may generate the hydrogen bond in the blends, restricting the movement of PBS segment. Thus, the crystallization of PBS segments may be restricted, and the reduced crystallinity facilitates the improvement of toughness of PBS. In this article, we mainly focus on the effect of hydrogen bonding on the structure, morphology, crystallization, as well as the mechanical properties of PBS/CDA blends. The Fourier transform infrared (FTIR), wide angle X-ray diffraction (WAXD), scanning electron microscope (SEM), polarizing optical microscope (POM), and differential scanning calorimeter (DSC) were used to characterize and confirm the hydrogen bonding interaction between PBS and CDA.

EXPERIMENTAL

Materials

Poly(butylene succinate) with a number-average molecular weight (M_n) of 100,000 g/mol was supplied by Hexing Chemical Company (Anhui, China). CDA was purchased from Sinopharm Chemical Reagent (Shanghai, China). Trifluoroacetic acid was purchased from Aldrich. Acetone and chloroform was purchased from Tianjin Damao Chemical Reagent Factory of China. All the reagents were used directly without further purification.

Preparation of PBS/CDA blends

To prepare the PBS/CDA blends, the PBS and CDA were dried under vacuum at 60°C for 24 h prior to use. Specified amounts of PBS and CDA were placed in a beaker; and the total amount of the materials was 1.0 g. Then, chloroform (20 mL), acetone (10 mL), and trifluoroacetic acid (5 mL) were added to the beaker. After being stirred vigorously for 24 h, the mixture became homogenous solution. The solu-

tion was cast onto a glass to obtain the films after the evaporation of solvents at room temperature. The weight ratio of PBS to CDA was designated as 90/10, 80/20, 70/30, 60/40, 50/50, 40/60, 30/70, 20/80, and 10/90, respectively.

Characterization

The Fourier transform infrared (FTIR) spectra were measured on a Shimadzu IRPrestige-21 FT-IR spectrophotometer.

The wide angle X-ray diffraction (WAXD) study was adopted to analyze crystalline structure of the samples by a Bruker D8 Focus X-ray diffractometer, operating at 30 kV and 20 mA with a copper target ($\lambda = 0.154$ nm) and in the 2θ angle range of 5–40° at a scanning rate of 0.5°/min.

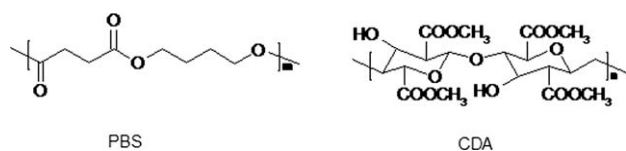
The surface and cross section morphology of the membranes were investigated by scanning electron microscope (SEM), using an Environmental Scanning Electron Microscope (ESEM, FEI Quanta 200F). All the samples were soaked in the liquid nitrogen and fractured, followed by the sputtering of a thin layer of gold. The surface and the cross section of the samples were then observed by the SEM with an accelerating voltage of 20 kV.

The melting and crystallization behaviors of the samples were performed on a Shimadzu DSC-60 calibrated with indium and zinc standards. The samples of about 5 mg were annealed at 170°C for 3 min to erase the thermal history. Then, the samples were cooled to –50°C at a rate of 10°C/min and subsequently heated to 170°C at a rate of 10°C/min. The crystallization and melting curves were recorded, and the corresponding glass transition temperature (T_g), crystallization temperature (T_c), melting temperature (T_m), crystallization enthalpy (ΔH_c), as well as the melting enthalpy (ΔH_m) were determined.

The crystal morphology of the samples was analyzed by a Nikon E600POL polarizing optical microscope (POM) equipped with an Instec HS 400 heating and cooling stage. The neat PBS and its blends were heated at 170°C for 3 min to erase the thermal history. Then, the samples were cooled to 25°C at the rate of 5°C/min. The PBS/CDA (80/20) sample was crystallized at different temperatures (45, 40, 35, 30°C) for 30 min after melting at 170°C for 3 min.

The thermal gravimetric analysis (TGA) was performed using a Perkin–Elmer instruments PYRIS DIAMOND at a heating rate of 10°C min⁻¹ under a nitrogen atmosphere (50 mL min⁻¹).

Tensile strength, elongation at break, and elastic modulus were measured with a CMT8502 Machine model GD203A (Shenzhen Sans Testing Machine, China) at a speed of 20 mm min⁻¹. The films prepared by the solution-casting method were cut into sheets of 50 × 25 mm with the thickness of about



Scheme 1 Structure of PBS and CDA.

0.05 mm. The strain gauge was used during the testing process. At least five specimens were tested for each sample, and the average values were reported.

A contact angle measurement JC2000A was used to measure static water contact angles of the polymer films at 25°C and 60% relative humidity using a sessile drop method. For each angle reported, at least five sample readings from different surface locations were averaged. The angles reported were reliable to $\pm 1^\circ$.

RESULTS AND DISCUSSION

Structure and morphology of PBS/CDA blends

The chemical structure of the PBS and CDA was shown in Scheme 1. FTIR was used to explore the structure of the PBS/CDA blends and possible interactions between PBS and CDA. As shown in Figure 1(A), it is observed that the PBS/CDA blends exhibit the similar absorption peaks except for the peaks at around 1750–1700 cm^{-1} region. The peak at 1712 cm^{-1} (C=O vibration) attributed to PBS shifts to higher wavenumbers and disappears at the content of 60% CDA. The neat CDA exhibits a peak at 1738 cm^{-1} , which is ascribed to the absorption of carbonyl group in CDA. Increasing of CDA content leads to the disappearance of the peak at 1712 cm^{-1} , showing that there is an interaction between the carbonyl groups of PBS and hydroxyl groups of CDA. In Figure 1(B), it is noticed that the PBS/CDA blends show additional peak at 1789 cm^{-1} except for the absorption of carbonyl groups of pristine PBS and CDA. The appearance of new peak might be related to the formation of hydrogen bond between PBS and CDA. It is suggested that the interactions between the hydroxyl groups in CDA and the carbonyl groups in PBS might lead to the formation of hydrogen bond. The existence of hydrogen bond is believed to improve the miscibility between PBS and CDA, and the crystallization of PBS will be restricted by the hydrogen bond interactions.

To explore the effect of CDA on the crystalline structure of PBS, WAXD analysis was performed to investigate the structure of PBS and PBS/CDA blends. Figure 2 shows the WAXD patterns of PBS and its blends. It is discerned that the pristine PBS exhibits the diffraction peaks at 2θ value of 19.8° and 22.7° . By increasing of the CDA content, the relative intensity of the reflection peaks decreases

significantly. At the CDA content above 60%, the reflection peak of the blend is not obviously observed. The phenomenon indicates that there should be some interactions between the PBS and CDA. Or else, the PBS should crystallize in its own regions and exhibit the reflection peaks in the X-ray spectra. Because of the physical blending between PBS and CDA, the formation of chemical bonds between PBS and CDA in the blends is impossible. As discussed above, the PBS contains the carbonyl groups and the CDA contains the hydroxyl groups in the molecular chains. The interactions between hydroxyl and carbonyl groups may lead to the formation of hydrogen bond. The existence of hydrogen bonding enhances the interaction between PBS and CDA, thus the miscibility was also improved. Additionally, the formation of hydrogen bond restricts the movement of PBS segment, making the crystallization of PBS difficult. Therefore, the reflection peaks of PBS crystals are not observed at high content of CDA due to the existence of hydrogen bonds.

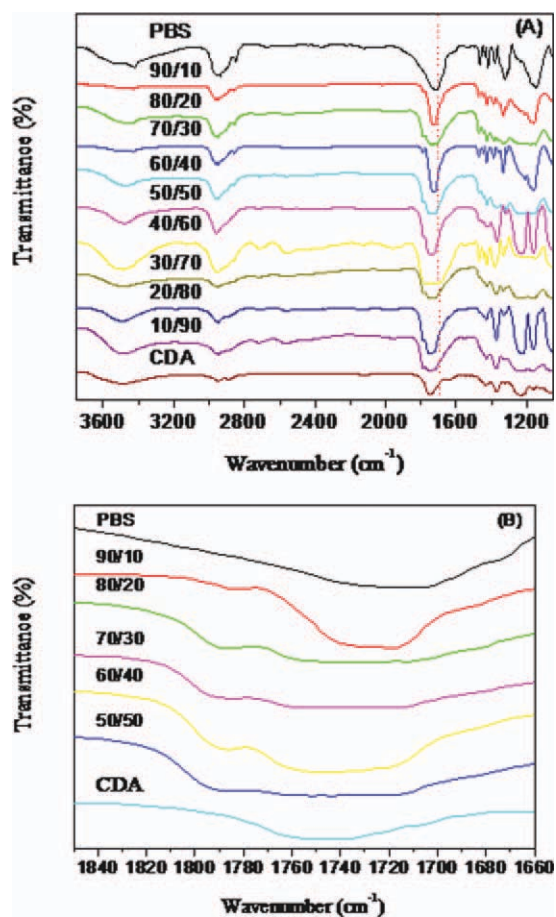


Figure 1 FTIR spectra of the films for (A) PBS, CDA, and PBS/CDA blends, (B) C=O stretching region from 1660 to 1850 cm^{-1} of PBS, CDA, and PBS/CDA blends. [Color figure can be viewed in the online issue, which is available at wileyonlinelibrary.com.]

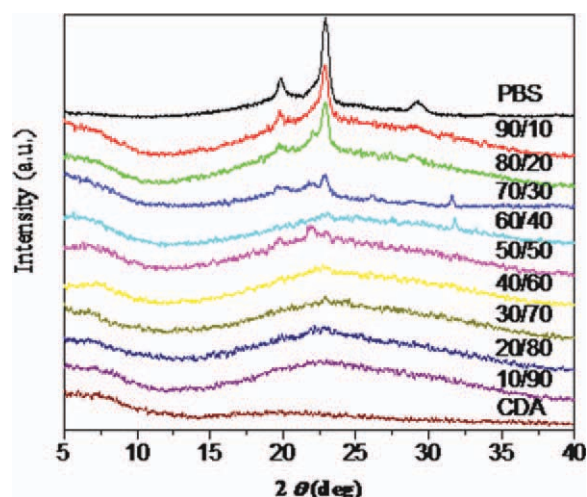


Figure 2 WAXD spectra of PBS and its blends. [Color figure can be viewed in the online issue, which is available at wileyonlinelibrary.com.]

The SEM graphs of the top surface and the fracture surface of neat PBS, CDA, and PBS/CDA (50/50) blend are shown in Figure 3. It is observed that the top surface of the blend is homogeneous without significant phase separation, indicating that the pristine PBS and CDA are compatible. Furthermore, the fracture surface of PBS is smooth, showing that the PBS is brittle after the treatment by liquid nitrogen. In comparison, the PBS/CDA blend shows of the rougher fracture surface, suggesting that the

sample becomes flexible. The neat CDA shows a much rougher fracture surface, attributed to the toughness of the CDA itself. The transition from brittleness to toughness of the samples is due to strong interaction between PBS and CDA molecular chains. As reported previously, CDA was flexible and could be used as the plasticizer in some polymers.^{19–21} Thus, the improved toughness of PBS is mainly due to the miscibility between PBS and CDA and the reduced crystallinity of PBS caused by the hydrogen bonding. Based on the SEM observation, it is revealed that PBS and CDA were miscible, and the incorporation of CDA improved the toughness of PBS.

Crystallization and spherulites morphology of PBS/CDA blends

Figure 4 shows the crystallization and melting curves of pristine PBS and its blend, and the corresponding data is illustrated in Table I. It is observed that one major crystallization peak for pristine PBS and 90/10 samples is discerned. The 80/20 sample exhibits double crystallization peaks, and the other samples show of no obvious crystallization peak at CDA content above 40%. The crystallization temperature of PBS shifts to lower values by the increase of CDA content, suggesting that the crystallization of PBS is strongly restricted by the incorporation of CDA component. Accordingly, the pristine

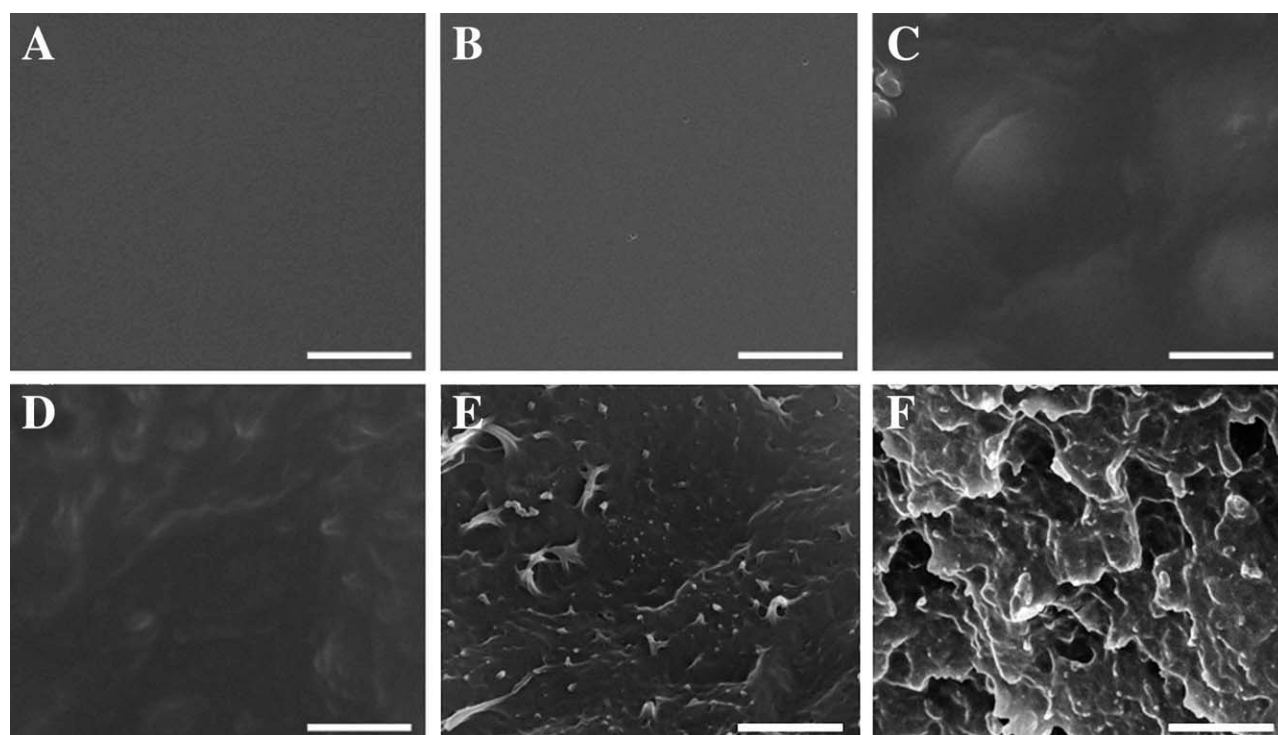


Figure 3 SEM graphs of surfaces of (A) PBS, (B) PBS/CDA (50/50) blend, and (C) CDA, respectively. The scale bar is 10 μm . The fracture surfaces of (D) PBS, (E) PBS/CDA (50/50) blend, and (F) CDA, respectively. The scale bar is 3 μm .

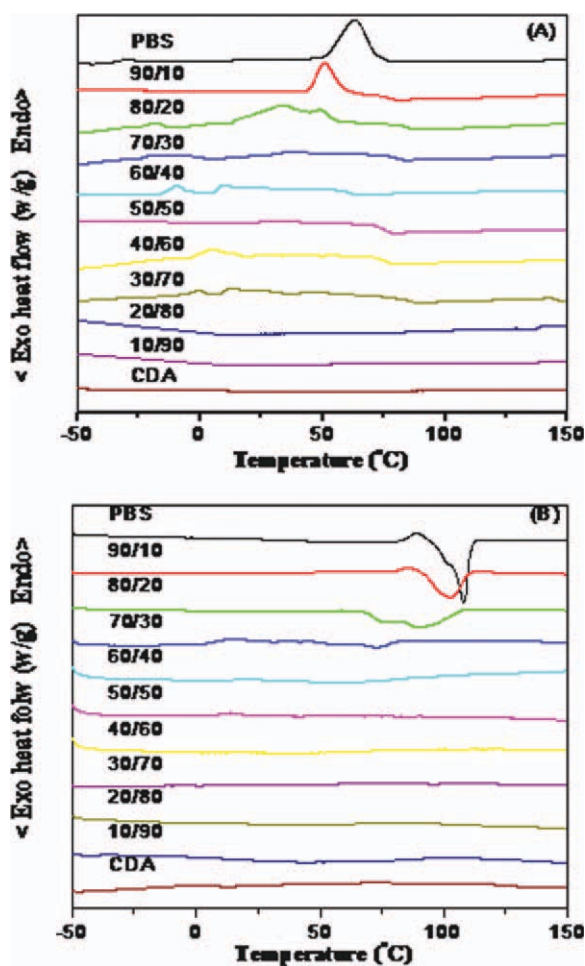


Figure 4 DSC cooling (A) and heating (B) curves for PBS and its blends. [Color figure can be viewed in the online issue, which is available at wileyonlinelibrary.com]

PBS, 90/10, 80/20, and 70/30 samples exhibit the melting peaks as observed in Figure 4(B), and the melting temperature decreases gradually with the increase of CDA content, showing that the incorporation of CDA leads to the formation of imperfect crystals in PBS. Furthermore, the crystallization and melting enthalpy of PBS is significantly reduced by blending with CDA as revealed in Table I. The values of T_g increase slightly with the increase of CDA content, showing that the mobility of PBS segment was also reduced by the CDA component. Based on the above results, it is indicated that the formation of hydrogen bond between the carbonyl groups in PBS and hydroxyl groups in CDA seriously affects the mobility of PBS molecular chains, leading to the enhanced glass transition temperature, reduced crystallization ability, as well as the low crystallinity. Similar results were also reported by Hashimoto,²⁵ in the blends of cellulose acetate butyrate (CAB) and poly(3-hydroxybutyrate) (PHB), the crystallization rate constant is strikingly reduced, which is attrib-

uted to physical crosslinks formed by intermolecular hydrogen bond between PHB and CAB in addition to molecular entanglements. Therefore, the restriction of crystallization of PBS matrix after the incorporation of CDA is mainly ascribed to the formation of physical crosslinks induced by the intermolecular hydrogen bond between PBS and CDA.

The polarizing optical microscope (POM) was further used to investigate the morphology of pristine PBS and its blends as shown in Figure 5. It is observed that the PBS, 90/10, 80/20, 70/30, 60/40, and 50/50 samples exhibit the maltese cross spherulites in the POM graphs. The interfaces of the spherulites are clear, and the graphs are full of PBS spherulites, showing of no significant phase separation between PBS and CDA. However, the diameter of PBS spherulites decreases by the addition of CDA, and the spherulites become less imperfect. It is suggested that the CDA component should be located in the lamellar or fibrillar regions of PBS, and CDA and PBS is compatible without significant phase separation due to the strong interactions between the components causing by hydrogen bond.

In Figure 6, the PBS/CDA (80/20) sample crystallized at different temperatures for 30 min shows spherulites of different morphology. The maltese cross of the spherulites becomes less obvious at lower temperature, indicating that the nucleating and crystal growth mechanism of the spherulites was affected by the incorporation of CDA. It is believed that the hydrogen bonding is stronger at lower temperatures. In this article, the mobility of PBS segment is relatively high at 45°C, showing of obvious maltese-cross spherulites due to the relatively weak hydrogen bonding. At lower temperature of 30°C, the mobility of PBS segment is believed to be reduced by the hydrogen bond. Thus, the crystallization of PBS is restricted, and the amorphous CDA should be located at its original region, leading to the formation of spherulites without obvious maltese cross. Instead, it is now replaced with dendritic bundles, which may be ascribed to presence of CDA molecules dissolving and reorienting the stereocomplexed spherulites into dendrites.²⁶ On the basis of the above result, it is suggested that the hydrogen bond played a vital role in determination of the morphology of PBS spherulites, as well as the crystallization mechanism of PBS.

TABLE I
DSC Data for PBS and Its Blends

PBS/CDA	T_g (°C)	T_m (°C)	T_c (°C)	ΔH_m (J/g)	ΔH_c (J/g)
100/0	-20.3	113.9	63.6	96.1	74.2
90/10	-11.6	102.8	50.8	36.5	41.8
80/20	-18.4	90.1	38.2	45.0	8.0
70/30	-17.0	73.0	22.4	12.9	12.0

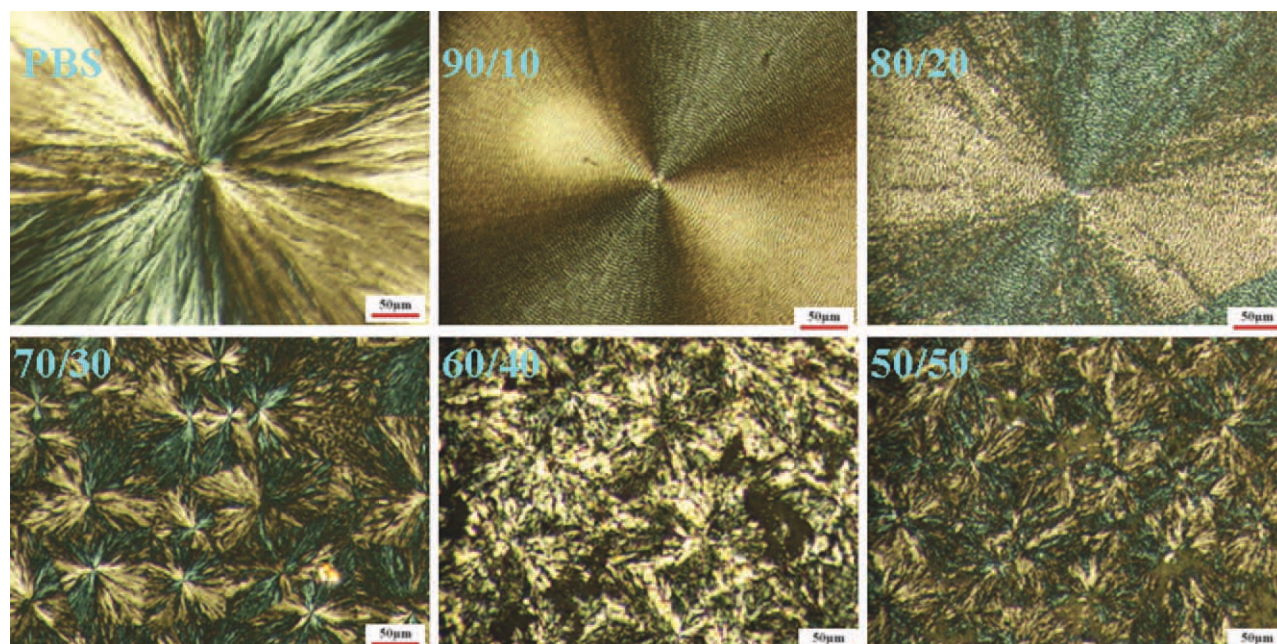


Figure 5 POM graphs of PBS/CDA blends cooling from 170 to 25°C at 5°C/min. [Color figure can be viewed in the online issue, which is available at wileyonlinelibrary.com.]

Thermal and tensile properties and water absorption of PBS/CDA blends

The thermal decomposition expressed in terms of weight loss as a function of the temperature for neat PBS, CDA, and PBS/CDA (50/50) blend is shown in

Figure 7. The onset degradation temperatures of the neat PBS and CDA are 156.6°C and 342.0°C, respectively. The blend exhibits a two-stage thermal decomposing behavior, which is corresponding to the decomposition of PBS and CDA components. If

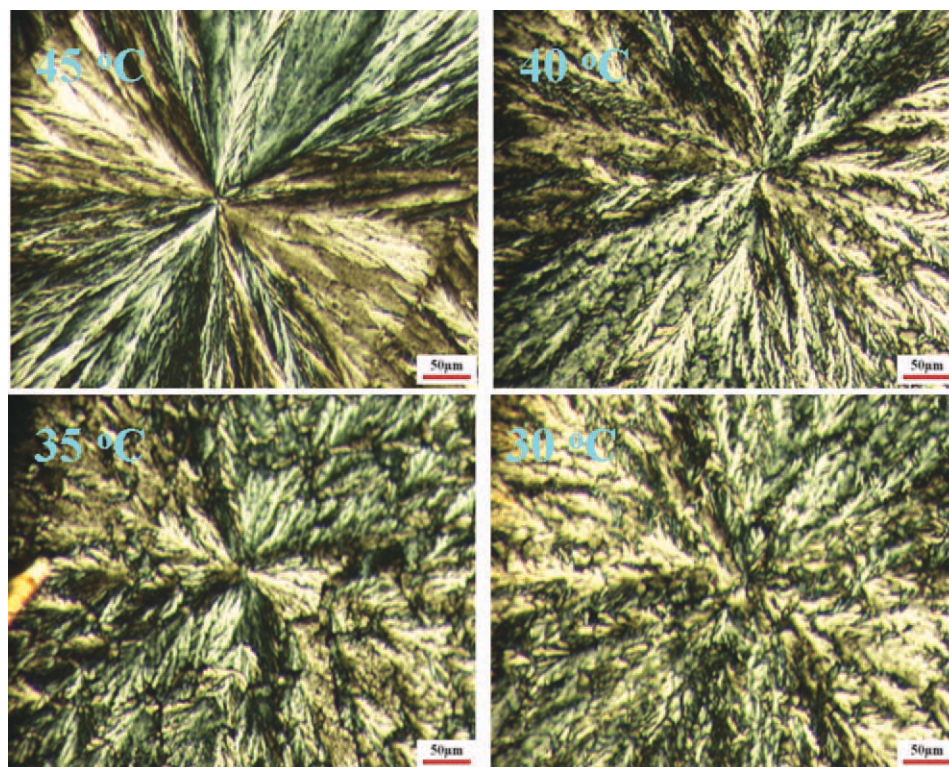


Figure 6 POM graphs of PBS/CDA (80/20) blend crystallized at different temperatures for 30 min. [Color figure can be viewed in the online issue, which is available at wileyonlinelibrary.com.]

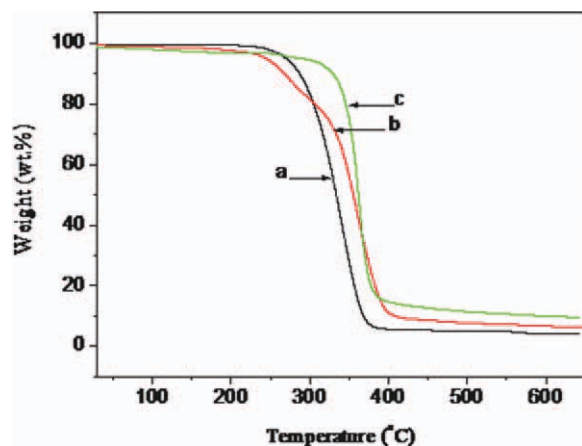


Figure 7 TGA curves of (A) PBS, (B) PBS/CDA (50/50) blend, and (C) CDA, respectively. [Color figure can be viewed in the online issue, which is available at wileyonlinelibrary.com.]

the two components in a blend have no interactions with each other, the TGA curve of the blend would show its thermal degradation in two stages matching with each component. In fact, the incorporation of CDA to PBS leads to the decomposition at lower temperature. It is suggested that a considerable interaction may exist between these components. The CDA is an amorphous component while the PBS is a crystalline one. The deep entanglement of the molecular chains in PBS/CDA blend reduced the crystallization of PBS due to the formation of hydrogen bond. Furthermore, the mechanical properties of PBS should be also affected by the formation of hydrogen bond.

To evaluate the effect of CDA on the mechanical properties of PBS, the tensile properties of PBS/CDA blend films were measured, and the corresponding results are illustrated in Table II. It is obviously observed that the elongation at break of PBS is significantly enhanced as the CDA content increases. However, both of the tensile strength and elastic modulus reduce with the increase of CDA content. It is suggested that the improvement of the flexibility of PBS may originate from the reduced crystallinity, as well as the toughness of CDA. In addition, the

TABLE II
Tensile Properties of PBS and Its Blends

PBS/CDA	Tensile strength (MPa)	Elongation at break (%)	Elastic modulus (MPa)
100/0	10.5 ± 2.2	6.4 ± 1.3	211.2 ± 5.6
80/20	4.9 ± 2.3	6.7 ± 1.5	175.3 ± 7.9
60/40	4.1 ± 1.2	9.2 ± 1.6	60.2 ± 5.7
50/50	8.0 ± 3.4	24.8 ± 1.4	67.5 ± 6.4
40/60	6.7 ± 1.3	30.8 ± 2.7	97.8 ± 8.3
20/80	7.7 ± 2.2	33.8 ± 3.2	53.1 ± 10.1
0/100	9.1 ± 2.6	52 ± 4.4	56.8 ± 12.1

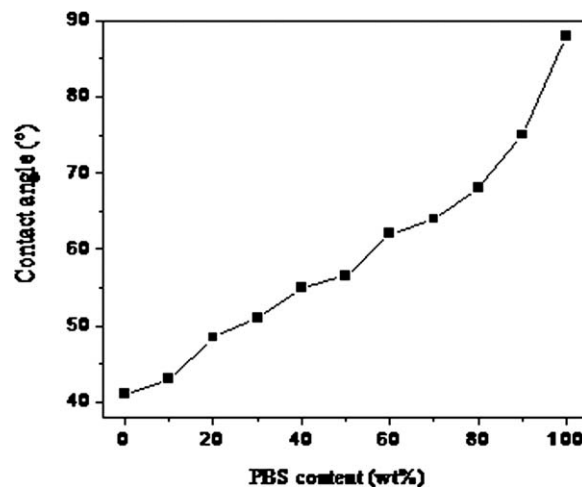


Figure 8 Contact-angle of PBS/CDA blend films with water versus PBS content.

decrease of tensile strength and elastic modulus of the samples is attributed to the decrease of PBS crystallinity, as well as the increase of CDA content. It is suggested that the hydrogen bond played a significant role in determination of the mechanical properties of the blends. The incorporation of CDA tended to improve the toughness of PBS due to the miscibility between CDA and PBS and reduced crystallinity of PBS caused by the hydrogen bonding.

As shown in Figure 8, the static water contact angle was measured to examine the hydrophilicity of the blend membranes. The neat PBS is determined to be about 88°, and the incorporation of CDA leads to the decrease of water contact of angle, showing that the hydrophilicity of the blend is significantly improved by the incorporation of the CDA due to the existence of large amount of hydroxyl groups in the molecular chains. The enhanced hydrophilicity might improve the applications of PBS in more areas.

CONCLUSIONS

Poly(butylene succinate)/cellulose diacetate (PBS/CDA) blends were prepared by the solution blending method from PBS and CDA. The existence of hydrogen bond significantly affected the structure, morphology, crystallization, as well as the physical properties of the PBS/CDA blends. The hydrogen bonding interaction between PBS and CDA was confirmed by the FTIR, XRD, DSC, and POM analysis. The formation of hydrogen bond restricted the crystallization of PBS segment due to the reduced flexibility of PBS molecular chains, as determined by X-ray, DSC, as well as POM analysis. The SEM graphs revealed that the PBS/CDA blend was miscible due to the hydrogen bonding, and the toughness

of PBS was improved by the incorporation of CDA. The thermal decomposing behavior and the tensile properties of PBS were also influenced by the existence of CDA, which is ascribed to the intermolecular interactions of hydrogen bond. The enhancement of elongation at break, as well as the reduction in tensile strength and elastic modulus is attributed to the decreased crystallinity of PBS and the toughness of CDA. The incorporation of CDA improved the hydrophilicity of PBS due to the hydroxyl groups in CDA.

References

1. Huda, M. S.; Drzal, L. T.; Misra, M.; Mohanty, A. K.; Williams, K.; Mielewski, D. F. *Industrial Eng Chem Res* 2005, 44, 5593.
2. Vink, E. T. H.; Rabago, K. R.; Glassner, D. A.; Gruber, P. R. *Polym Degrad Stabil* 2003, 80, 403.
3. Avella, M.; Errico, M.; Laurienzo, P.; Martuscelli, E.; Raimo, M.; Rimedio, R. *Polymer* 2000, 41, 3875.
4. Ray, S. S.; Okamoto, K.; Okamoto, M. *Macromolecules* 2003, 36, 2355.
5. Witte, P.; Esselbrugge, H.; Dijkstra, P.; Berg, J. W. A.; Feijen, J. *J Polym Sci, Part B: Polym Phys* 1996, 34, 2569.
6. Song, J.; Ren, M.; Chen, Q.; Sun, X.; Zhang, H.; Song, C.; Mo, Z. *J Polym Sci Part B: Polym Phys* 2005, 43, 2326.
7. Fernandes, E. G.; Pietrini, M.; Chiellini, E. *Biomacromolecules* 2004, 5, 1200.
8. Harada, M.; Ohya, T.; Iida, K.; Hayashi, H.; Hirano, K.; Fukuda, H. *J Appl Polym Sci* 2007, 106, 1813.
9. Nugroho, P.; Mitomo, H.; Yoshii, F.; Kume, T.; Nishimura, K. *Macromol Mater Eng* 2001, 286, 316.
10. Sinha Ray, S.; Bousmina, M. *Macromol Rapid Commun* 2005, 26, 1639.
11. Valadez-Gonzalez, A.; Cervantes-Uc, J.; Olayo, R.; Herrera-Franco, P. *Composites Part B: Eng* 1999, 30, 309.
12. Mohanty, A.; Misra, M.; Drzal, L. *J Polym Environment* 2002, 10, 19.
13. Lnnberg, H.; Zhou, Q.; Brumer, H.III; Teeri, T. T.; Malmstr m, E.; Hult, A. *Biomacromolecules* 2006, 7, 2178.
14. Klemm, D.; Heublein, B.; Fink, H. P.; Bohn, A. *Angewandte Chemie Int Ed* 2005, 44, 3358.
15. Edgar, K. J.; Buchanan, C. M.; Debenham, J. S.; Rundquist, P. A.; Seiler, B. D.; Shelton, M. C.; Tindall, D. *Prog Polym Sci* 2001, 26, 1605.
16. Czaja, W.; Krystynowicz, A.; Bielecki, S.; Brown, R. M. *Biomaterials* 2006, 27, 145.
17. George, J.; Ramana, K.; Bawa, A.; Siddaramaiah, B. *Int J Biol Macromol* 2011, 48, 50.
18. Iguchi, M.; Yamanaka, S.; Budhiono, A. *J Mater Sci* 2000, 35, 261.
19. Lee, C. K.; Cho, M. S.; Kim, I. H.; Lee, Y.; Nam, J. D. *Macromol Res* 2010, 18, 566.
20. Ogata, N.; Tatsushima, T.; Nakane, K.; Sasaki, K.; Ogihara, T. *J Appl Polym Sci* 2002, 85, 1219.
21. Sundar, S.; Sain, M.; Oksman, K. *JThermal Analysis Calorimetry* 2011, 1.
22. Uesaka, T.; Nakane, K.; Maeda, S.; Ogihara, T.; Ogata, N. *Polymer* 2000, 41, 8449.
23. Uesaka, T.; Ogata, N.; Nakane, K.; Shimizu, K.; Ogihara, T. *J Appl Polym Sci* 2002, 83, 1750.
24. Tachibana, Y.; Giang, N. T. T.; Ninomiya, F.; Funabashi, M.; Kunioka, M. *Polym Degrad Stabil* 2010, 95, 1406.
25. Suttiwijitpukdee, N.; Sato, H.; Zhang, J.; Hashimoto, T. *Macromolecules* 2011, 44, 3467.
26. Chang, L.; Woo, E. M. *Polymer* 2011, 52, 68.